RC 1

The manuscript presents a comprehensive (counting over 3,500 landslides) multi-temporal landslide inventory for the Collazzone area (central Italy), covering more than 80 years of observations derived from different datasets.

The long-term continuity of the dataset, the rigorous mapping procedures, and the integration of heterogeneous sources make this inventory a valuable contribution for hazard assessment, geomorphological analysis, and landscape evolution studies. Overall, the work is scientifically solid, methodologically robust, and highly useful for the community. Only minor revisions are needed to improve clarity, readability, and metadata completeness.

MAIN COMMENTS

1. The manuscript would benefit from a clearer explanation of how the different mapping scales and data sources were harmonized when delineating landslide polygons. The criteria used to define polygon boundaries in relation to the different dataset scales are not fully described, and the handling of spatial and temporal uncertainties, particularly for inter-survey periods, could be explicitly detailed.

   Rows 154-163: The landslides observed in the field and delineated as polygons on Google Earth imagery, those identified through visual interpretation of very high-resolution (VHR) optical stereo satellite images and mapped directly on-screen (Ardizzone et al., 2013; Murillo-García et al., 2015), and those recognized through systematic inspection of the imagery available in Google Earth were mapped at a level of detail greater than that achievable at a 1:10,000 scale. This higher level of detail applies both to the minimum size of the mapped landslides and to the accuracy of the delineated polygon boundaries. Ardizzone et al., 2007 demonstrated that improved topographic information significantly enhances landslide identification and delineation. Consequently, the multi-temporal inventory is characterized by two different mapping scales. Until 2005, landslides were represented according to the cartographic scale of 1:10,000. After 2005, the effective mapping scale was controlled by the resolution of the VHR satellite imagery and Google Earth images used for landslide identification and mapping, resulting in a substantially finer level of detail.

   Rows 198-216: The recognition of geomorphological features from stereoscopic aerial photographs requires experience, training, a systematic methodology, and well-defined interpretation criteria (Zuidam and Zuidam-Cancelado, 1986). Photo interpreters classify geological objects and landforms based on their expertise and on the analysis of a set of diagnostic characteristics that can be identified in photographic imagery. These include shape, size, photographic color, tone, mottling, texture, pattern of objects, site topography and setting (Antonini et al., 2002; Murillo-García et al., 2015; Richard G. Ray, 1960). Shape refers to the form of the topographic surface. Due to the vertical exaggeration of stereoscopic vision, shape is the most useful characteristic for the classification of an object from aerial photographs. Size describes the area extent of an object. Knowing the physical dimensions of an object is seldom enough for classification, but it can be very useful to identify properties such as extent and depth. Color, tone, mottling and texture depend on the light reflected by the surface, and can be used to infer rock, soil and vegetation types, the latter being a proxy for wetness. Mottling and texture are measures of terrain roughness and can be used to identify surface types and the size of debris. Pattern is the spatial arrangement of objects in a repeated or characteristic order or form and is used to infer rock type and resistance to erosion, as well as the presence of faults and other tectonic lineaments. Topographic site is the position of a place with reference to its surroundings. It reflects morphometric characteristics such as height difference, slope steepness and aspect, and the presence of convexities or concavities in the terrain. Setting expresses regional and local characteristics (lithological, geological, morphological, climatic, vegetational, and so on) in relation to the surroundings. Site topography and setting are particularly suited to inferring rock type and structure, attitude of bedding planes, and presence of faults and other tectonic features. Extensive field checks were conducted to check the landslides mapped.

Rows 221-226: Old and very old landslides (i.e., those occurring before 1941) are typically characterized by vegetation recolonization and by the dissection of the landslide topography by drainage networks (Cruden and Varnes, 1996). Landslides that occurred from 1941 onwards can be identified through the presence of scarps and deposit zones, as well as by changes in vegetation patterns. "Fresh" slope failures were assigned the date (i.e., the year) corresponding to the aerial photographs in which they were first identified (i.e. 1941, 1954, 1977, 1985, 1997). These "fresh" landslides are characterized by colour, tone, and texture contrasts relative to the surrounding undisturbed terrain.

2. It is not clear whether the authors explored any relationship between mapped landslides and potential meteorological triggers. Including a long-term precipitation plot (e.g., 1940-2023) would help visualise temporal correspondence, uncertainties, and possible triggering conditions associated with each mapping period.

   Rows 101-108: Landslides are abundant and are caused primarily by meteorological triggers, including prolonged rainfall and rapid snowmelt (January 1997), no historical information of earthquake-induced landslides exists for the study area (https://sici.irpi.cnr.it/). Appendix B presents a histogram of the cumulative monthly rainfall and mean monthly precipitation recorded at the Todi rain gauge (location shown in Fig. 1A) for the period 1940–2023. The mean annual rainfall during this period is approximately 849 mm. The histogram also displays, as black dots, the dates corresponding to the landslide inventory layers (Table 1). Ardizzone et al., 2007, 2013; Fiorucci et al., 2011 investigated the rainfall conditions associated with landslides triggered by precipitation events occurring after 2000, whereas examined the snowmelt event that affected the Umbria Region in 1997 and triggered numerous landslides, including several within the study area (E_2 in Table 1).

3. The structure of the database and metadata could be presented in greater detail. A schematic representation of the database, a list of attribute fields with their domains would benefit the reproducibility.

   The structure of the database was added in Appendix-A (annexed to the response).

   Figures 3 and 4 are difficult to interpret due to the colour scheme, which does not follow a clear temporal logic. A more structured chromatic progression would improve readability.

   Figures 3 and 4 have been modified as requested. Since landslides mapped after 1997 were identified using different methods than those used for earlier periods, and because they are fewer and generally smaller in size, they have been highlighted using brighter colours for improved visibility. The colour scheme was therefore revised based on the mapping technique (field surveys, VHR satellite imagery, and Google Earth imagery), with colours becoming progressively darker over time within each group. We hope that the revised figures adequately address the reviewer's request. Figure 5 has also been updated accordingly.

MINOR ISSUES

4. LINE 8: Replace with "multi-temporal" and ensure consistency throughout the text.

   I have done it.

5. LINE 10: Clarify the meaning of "the build environment"; do you refer to infrastructures or the built environment more broadly?

   I have changed the word in structure and infrastructure.

6. LINE 33: “Vintages” may not be the most appropriate term; consider rephrasing.

   I have changed the word in age.

7. LINE 55: Correct “(Bhutyan et al., 2023a)”.

   I have done it.

8. LINE 58: The study area should be explicitly mentioned here and also in the abstract.

   I have done it.

9. LINES 75–77: Consider anticipating the age information as “Plio-Pleistocene continental gravel, sand and clay”.

   I have done it.

10. EQUATION 1: Replace “con” and correct the condition to $0 \leq E \leq 1$.

    I have done it.

APPENDIX-A

The digital multitemporal landslides inventory map is composed of 29 polygon shapefiles (Table 1). The EPSG is 23033. The attribute table of each shapefile includes three fields, beyond the default fields: N, CODE and LEGEND (Table 2). Table 3 shows the legend of the types of landslides.
The 29 shape files named as the layer in table 1 and the corresponding geopackage named “Landslide_inventory_Collazzone.gpkg” are available in ZENODO repository (https://zenodo.org/records/18980281).

LAYER	LANDSLIDE NUMBER	ESTIMATED LANDSLIDE AGE	TYPE OF SURVEY
A_0	27	very old, relict	P-I
A_1	269	older than 1941	P-I
A_2	706	1941	P-I
B_1	63	1941–1954	P-I
B_2	97	1954	P-I
C_1	408	1954-1977	P-I
C_2	251	1977	P-I
D_1	105	1977-1985	P-I
D_2	135	1985	P-I
E_1	63	1985-1997	P-I
E_2	411	1997	P-I
F_1	17	1999-2000	F-S
F_2	70	May 2004	F-S
F_3	168	December 2004	F-S
F_4	60	December 2005	F-S
G_1	161	Sept-Mar 2010	S-I-I
G_2	55	Apr-May 2010	S-I-I
G_3	1	April 2011	G-E-I
G_4	6	May 2012	G-E-I
G_5	108	April 2013	S-I-I
G_6	217	April 2014	S-I-I
G_7	103	March 2015	G-E-I
G_8	14	July 2015	G-E-I
G_9	16	April 2018	G-E-I
G_{10}	14	October 2019	G-E-I

F_5	21	December 2020	F-S
G_{11}	128	April 2021	G-E-I
G_{12}	3	March 2022	G-E-I
G_{13}	3	May 2023	G-E-I

Table 1 – Shapefiles included in the multi-temporal landslide inventory map. P-I: Photo Interpretation; F-S: Field Survey; S-I-I: Satellite Image Interpretation; G-E-I: Google Earth Image interpretation.

FIELD	DATA TYPE	LENGHT	DESCRITPION
N	Long Integer	-	Landslide Identification number
CODE	Text	10	The type of landslide movement. The field takes the value shown in table 3.
LEGEND	Text	50	Extended legend of the type of landslide movement. The field takes the value shown in table 3.

Table 2 – List of the fields included in the attribute table of each shapefile of the multi-temporal landslide inventory map of Collazzone study area. The table includes three fields beyond the default fields: N, CODE and LEGEND.

Landslide type		
CODE	**LEGEND**	**DESCRIPTION**
s	Slide	Slides are movements that produce general concavities and convexities of the topographic surface without significant disarticulation. The slip surface can range from very shallow (affecting only the soil horizons) to very deep. In the case where the geomorphological evidence has not allowed the identification of the escarpment, the landslide is represented without escarpment and is to be considered superficial. Where the escarpment has been recognized, it has been represented with a polygon distinct from that relating to the deposit.
x_s	Slide escarpment	Escarpment of slide type movement.
f	Earth flow	Earth flows involve predominantly clay, plastic materials, generally on slopes that are not very steep. They have narrow and elongated shapes characterized by a generally narrow and elongated channel and by an accumulation that at the foot assumes the characteristic fan shape in plan, and convex in section. Where the escarpment has been recognized, it has been represented with a polygon distinct from that relating to the deposit.

x_f	Earth flow escarpment	Escarpment of earth flow type movement.
sef	Slide-earth flow	Movements start as slides and then evolve into flows. Therefore, they show the characteristics of slides. Where the escarpment has been recognized, it has been represented with a polygon distinct from that relating to the deposit.
x_sef	Slide-earth flow escarpment	Escarpment of slide-earth flow type movement.

Table 3 – Legend according to Cruden & Varnes, 1996 [Cruden, D.M. and Varnes, D.J., 1996. Landslides: investigation and mitigation. Chapter 3-Landslide types and processes. Transportation research board special report, (247)].

APPENDIX-B

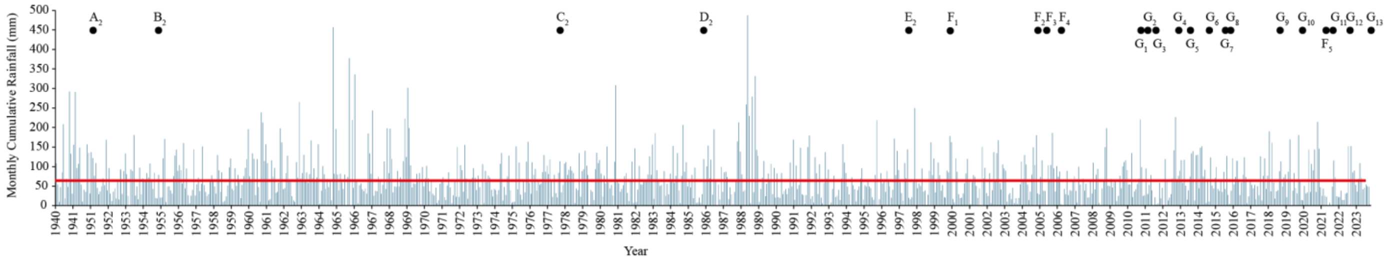

The graph shows the monthly cumulative rainfall (mm) measured at Todi rain gauge (Fig. 1A) from 1940 to 2023. The red line indicates the average annual rainfall equal to 72 mm. The black dots A_2, B_2, C_2, D_2, and E_2 show the date of the stereophotographs. The black dots F_1, F_2, F_3, F_4 and F_5 show the date of the field surveys. The black dots G_1, G_2, G_5 and G_6 show the date of the very high-resolution satellite images. The black dots G_3, G_4, G_7, G_8, G_9, G_{10}, G_{11}, G_{12} and G_{13}, show the date of the Google Earth Pro images.